

Communication: “Position” does matter: The photofragmentation of the nitroimidazole isomers

Cite as: J. Chem. Phys. **145**, 191102 (2016); <https://doi.org/10.1063/1.4967770>

Submitted: 28 September 2016 • Accepted: 01 November 2016 • Published Online: 21 November 2016

 P. Bolognesi, A. R. Casavola,  A. Cartoni, et al.



View Online



Export Citation



CrossMark

ARTICLES YOU MAY BE INTERESTED IN

[A joint theoretical and experimental study on diiodomethane: Ions and neutrals in the gas phase](#)

The Journal of Chemical Physics **143**, 244312 (2015); <https://doi.org/10.1063/1.4937425>

[Time-of-Flight Mass Spectrometer with Improved Resolution](#)

Review of Scientific Instruments **26**, 1150 (1955); <https://doi.org/10.1063/1.1715212>

[Vibrationally resolved high-resolution NEXAFS and XPS spectra of phenanthrene and coronene](#)

The Journal of Chemical Physics **141**, 044313 (2014); <https://doi.org/10.1063/1.4891221>

[Learn More](#)

The Journal of Chemical Physics **Special Topics** Open for Submissions

Communication: “Position” does matter: The photofragmentation of the nitroimidazole isomers

P. Bolognesi,^{1,a)} A. R. Casavola,^{1,a)} A. Cartoni,^{1,2} R. Richter,³ P. Markus,¹ S. Borocci,⁴ J. Chiarinelli,¹ S. Tošić,⁵ H. Sa'adeh,⁶ M. Masič,⁷ B. P. Marinković,⁵ K. C. Prince,³ and L. Avaldi¹

¹*CNR-Istituto di Struttura della Materia, Area della Ricerca di Roma1, Monterotondo, Italy*

²*Dipartimento di Chimica, Sapienza Università di Roma, Roma, Italy*

³*Elettra-Sincrotrone Trieste, Basovizza, Italy*

⁴*Dipartimento per l'Innovazione nei Sistemi Biologici, Agroalimentari e Forestali (DIBAF), Università della Tuscia, Viterbo, Italy*

⁵*Institute of Physics Belgrade, University of Belgrade, Belgrade, Serbia*

⁶*Department of Physics, The University of Jordan, Amman, Jordan*

⁷*School of Chemistry, Cardiff University, Cardiff, United Kingdom*

(Received 28 September 2016; accepted 1 November 2016; published online 15 November 2016)

A combined experimental and theoretical approach has been used to disentangle the fundamental mechanisms of the fragmentation of the three isomers of nitroimidazole induced by vacuum ultra-violet (VUV) radiation, namely, 4-, 5-, and 2-nitroimidazole. The results of mass spectrometry as well as photoelectron–photoion coincidence spectroscopy display striking differences in the radiation-induced decomposition of the different nitroimidazole radical cations. Based on density functional theory (DFT) calculations, a model is proposed which fully explains such differences, and reveals the subtle fragmentation mechanisms leading to the release of neutral species like NO, CO, and HCN. Such species have a profound impact in biological media and may play a fundamental role in radiosensitising mechanisms during radiotherapy. *Published by AIP Publishing.* [<http://dx.doi.org/10.1063/1.4967770>]

Radiotherapy using different radiation sources like photons, electrons, and ion beams, has represented a major improvement in cancer treatment. Nevertheless, its lack of selectivity in the induced damage is still a serious drawback. Thus, a major issue in oncology therapy¹ is to devise tools to enhance the effects of radiation on tumour cells while minimising the damage to adjacent healthy tissues. An enhancement of the radiation damage² can be triggered directly in the DNA of tumour cells by selective incorporation of DNA base analogues,³ for example, or indirectly, via radiation induced secondary processes leading to the release of free electrons⁴ and reactive species, as well as oxygen and “oxygen mimetic” compounds.⁵ Indeed hypoxia, which is a consequence of the inefficient vascularisation of some tumours, favours the metabolism and growth of tumour cells and makes them more resistant to radiotherapy⁶ than the ones in a normally oxygenated environment. In this respect oxygen is a potent radiosensitiser.⁵ Nitric oxide has long been recognized for its effects in tumour reoxygenation^{7–9} and has been considered an even more efficient radiosensitiser than oxygen itself [see, for example, Ref. 10 and references therein]. The understanding of these radiosensitising mechanisms is of fundamental importance in the design and characterisation of novel drugs, reducing the risk of negative trials.^{11,12}

2- and 5-nitroimidazole (C₃H₃N₃O₂, m = 113 amu) isomers, i.e., derivatives of imidazole containing one nitro group

are, respectively, the building blocks of misonidazole and nimorazole radiosensitisers used in clinical trials as “oxygen mimetic” compounds.^{5,13} They increase the effectiveness of a given dose of radiation by reacting with radiation induced DNA radicals and reducing the DNA repairing capabilities⁹ in otherwise resistant hypoxic tumour cells. In clinical trials, the 2-nitroimidazole drug appeared to be more effective than the 5-nitroimidazole one.^{2,12} The fundamental reasons for such different behaviour are not yet understood and even though these drugs have a certain level of toxicity, there are still ongoing clinical trials aiming to refine the use of nimorazole.¹² In this work we present a joint experimental and theoretical study of the radiation induced fragmentation of 4-, 5-, and 2-nitroimidazole isomers, providing clear evidence of their different fragmentation patterns. The results suggest that particular products of their decomposition may influence the effectiveness of the radiosensitising action of their derivatives.

The experiments are based on the photofragmentation of isolated 4(5)- and 2-nitroimidazole molecules by the tunable synchrotron radiation of the GasPhase photoemission beamline^{14–16} at Elettra (Trieste, Italy) and the vacuum ultra-violet (VUV) radiation of a rare gas discharge lamp.¹⁷ The setups have been described elsewhere^{14,17} and more details are reported in the [supplementary material](#). Briefly, the end station at Elettra consists of a 150 mm mean radius hemispherical electron energy analyzer (VG 220i) mounted opposite to a time of flight (TOF) spectrometer, operated in pulsed extraction mode. The electron and ion mass analysers can be operated independently, for photoelectron and mass spectroscopy

^{a)}Authors to whom correspondence should be addressed. Electronic addresses: paola.bolognesi@cnr.it and annarita.casavola@cnr.it

measurements, or simultaneously in photoelectron–photoion coincidence (PEPICO) experiments. In this PEPICO mode, ion-state selected mass spectra can be measured, where the fragmentation pattern following the ionization from a specific molecular orbital is directly accessed. In the experiments with the discharge lamp, the TOF spectrometer is operated with continuous extraction. The target molecules, 4- and 2-nitroimidazole, were purchased from Sigma Aldrich, with a specified purity of 97% and 98%, respectively. They are in the form of powders at ambient temperature and atmospheric pressure. Therefore they were introduced into the vacuum chamber in a crucible and heated to about 80 °C to be sublimated for gas phase analysis. The 4-nitroimidazole (4NI) and 5-nitroimidazole (5NI) are regioisomers that differ in the position of the H atom on either of the two N atoms within the imidazole ring (see inset in Figure 1) and are almost degenerate in energy. The 4NI isomer was found to be more stable than 5NI in water¹⁸ and in the crystalline state,¹⁹ while in the gas phase they coexist in a tautomeric equilibrium.¹⁸ XPS measurements together with density functional theory (DFT) based theoretical calculations by Feketeová *et al.*²⁰ found a relative population of 1:0.7 for the 4NI:5NI molecules at 117 °C. Therefore, in the following, we will refer to the 4(5)NI sample assuming that both isomers coexist in gas phase experiments. The fragmentation mass spectra of the 4(5)NI and 2NI molecules measured at 60 eV photon energy and the assignment of the main fragmentation channels are shown in Figure 1.

The two samples display many similar features and relative intensities, but also a few intriguing peculiarities. The most striking differences are observed in the fragments at m/z 55⁺ and 56⁺, present exclusively in 4(5)NI and 2NI, respectively, and the fragment at m/z 83⁺, which is one of the leading fragmentation channels in 2NI, but is almost absent in the 4(5)NI sample. Such differences were also observed in electron impact experiments.²¹ The peaks at m/z 55⁺ and 56⁺

can be attributed to the loss of CNO₂ and HCN₂O, respectively, while the m/z 83⁺ fragment can be unambiguously attributed to the loss of nitric oxide. The latter is particularly relevant for its potential implications in the biological context because of the well proven and recognised action of NO as radiosensitiser and vasodilator.⁹

Further support for these observations is provided by the PEPICO measurements. In Figure 2, the yield of each fragment is reported versus the binding energy of the valence orbital ionised. The corresponding photoelectron spectrum, also reported in Figure 2, is composed of two broad features resulting from the ionisation of the lower binding energy orbitals.²⁰ Apart from the parent ion observed at the ionization threshold and over the first band, the PEPICO spectra show that, within the experimental energy resolution of the coincidence measurements, several fragmentation channels open up almost simultaneously at a binding energy of about 10.7 eV, i.e., in the second band of the photoelectron spectrum, and display similar trends versus binding energy. At variance with the previously studied six membered ring molecules,^{15,22} the nitroimidazoles display little state-selectivity in the fragmentation of these low-energy molecular orbitals. The main observation in Figure 2 is that fragments at m/z 83⁺ and 30⁺ dominate in 2NI, while m/z 28⁺ and 55⁺ fragments dominate in 4(5)NI. These observations are completely consistent with those of the mass spectra of Figure 1.

At first glance, the experimental spectra in Figures 1 and 2 may lead to the conclusion that 2NI releases a significant amount of NO, while 4(5)NI does not, explaining the enhanced performance of 2NI as a radiosensitiser. However, previous theoretical calculations²⁰ revealed very similar energetics for the NO-loss channel in the three isomers, suggesting that a more complex description is needed to explain the results. Thus, in order to explain these differences in the photofragmentation of nitroimidazole isomer radical cations, we have performed new theoretical calculations on the three

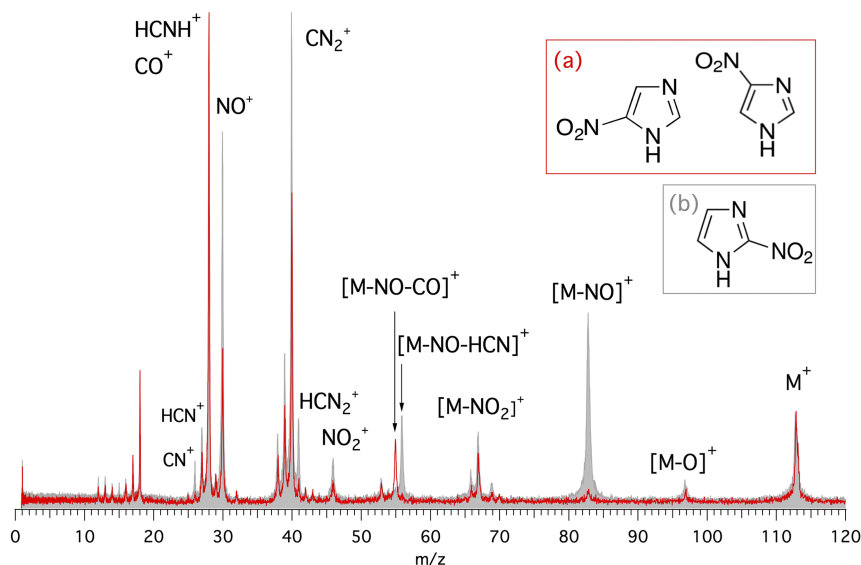


FIG. 1. Mass spectra of 4(5)-nitroimidazole (red line and inset (a)) and 2-nitroimidazole molecules (gray, full, area and inset (b)) measured at 60 eV photon energy. The assignment of the main fragments is reported. Clear differences can be observed in the intensity of fragments m/z 83⁺, 56⁺, and 55⁺, as well as m/z 30⁺ and 28⁺. These specific fragmentation channels are discussed in the text. All masses are in amu.

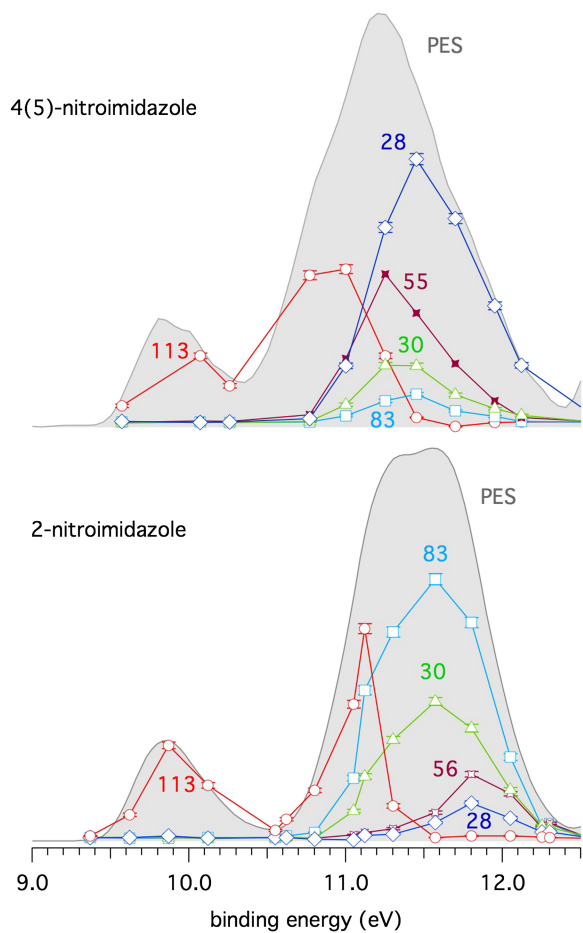


FIG. 2. PES (grey full area) and PEPICO spectra (coloured lines) of selected fragments of 4(5)- and 2-nitroimidazole measured at 60 eV photon energy. In these measurements, the kinetic energy of the photoelectron identifies the binding energy of a specific molecular orbital so that the mass spectrum measured in coincidence corresponds to the fragmentation of that specific electronic state. Here the intensities of all the fragments present in the measured PEPICO spectra are reported versus binding energy.

molecules, focusing on the NO and CO-loss pathways. A more extensive study, including other fragmentation channels and photoelectron spectroscopy, will be presented in a further publication.

All calculations were performed using Gaussian 09.²³ The geometries were optimized at the level of Density Functional Theory (DFT). In particular, the Becke, three-parameter, Lee-Yang-Parr (B3LYP) functional and the 6-311++G** basis set were used. The frequency analysis was based on the normal mode harmonic approximation.²⁴ Accurate total energies were obtained by single-point coupled cluster calculations, CCSD,²⁵ using the same basis sets for the B3LYP calculations. The CCSD T1 diagnostic is within the recommended threshold of 0.02,²⁶ suggesting that these species are correctly described by a single-reference method. All critical points were characterized as energy minima or transition structures (TS) by calculating the corresponding B3LYP harmonic frequencies, also used to evaluate the zero-point energy correction. The TS were unambiguously related to their interconnected energy minima by intrinsic reaction coordinates (IRC) calculations (see the [supplementary material](#)).^{27,28}

The resulting potential energy surfaces for the fragmentation of the 4NI, 5NI, and 2NI radical cation isomers are reported in Figures 3(a)–3(c). In all isomers the most stable structure of the radical cation corresponds to a quasi-planar arrangement with the nitro group out of the plane with respect to the neutral molecule (see the [supplementary material](#)). This structure allows the easy NO-loss following an intramolecular rearrangement in the nitro group, with energy barriers of 1.35,

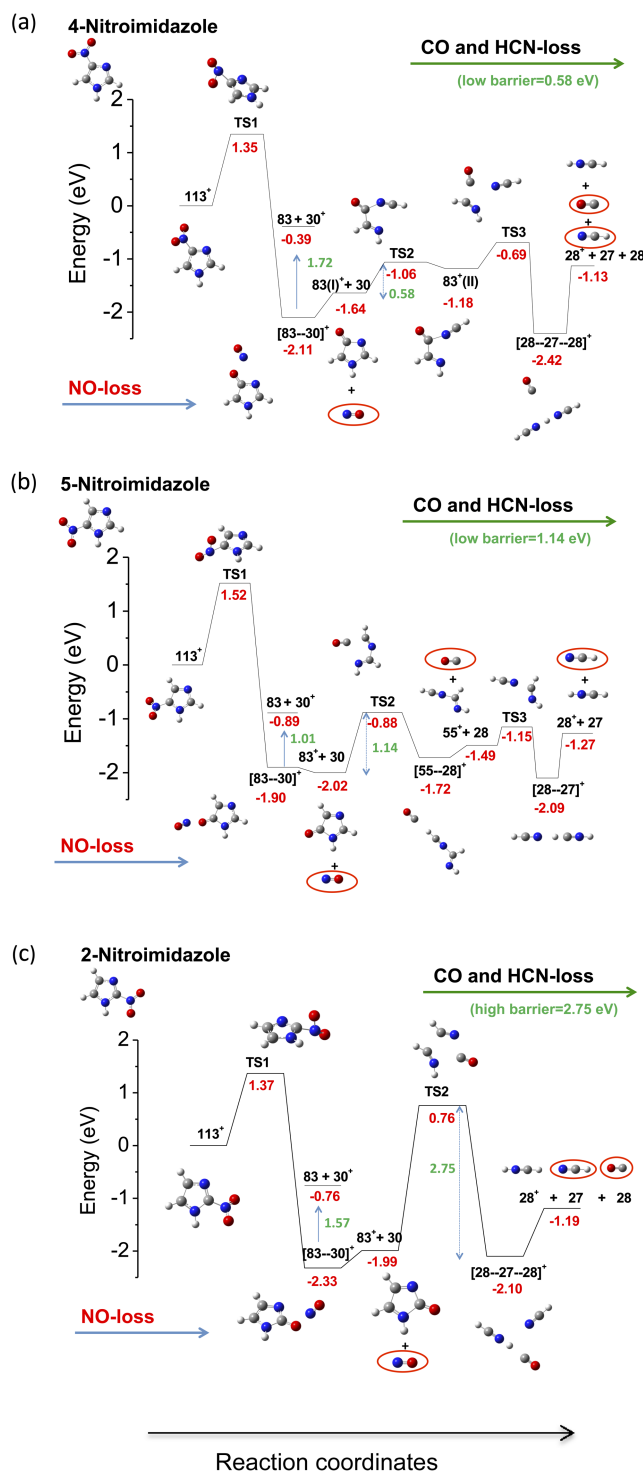


FIG. 3. Potential energy profiles for 4-, 5-, and 2-nitroimidazole (with zero point energy, ZPE) calculated at the CCSD//B3LYP level for the fragmentation of their corresponding molecular ions $[M]^+$ (m 113 amu). The energy is the sum of the energies of the products relative to that of the radical cation $[M]^+$.

1.52, and 1.37 eV for 4NI, 5NI, and 2NI, respectively. The second oxygen atom remains bound to the corresponding C atom in the ring. In all isomers, the NO-loss from the $[83-30]^+$ adduct can produce the $C_3H_3N_2O^+$ ion at m/z 83⁺, which preserves the ring structure, or the NO^+ ion at m/z 30⁺. From the energetic point of view, the three isomers show a very similar behaviour in the formation of the 83⁺ fragment, while the subsequent fate of the m/z 83⁺ ions is profoundly different. In 4NI (Figure 3(a)), the intermediate 83⁺ fragment is unstable and, by overcoming an energy barrier of only 0.58 eV (TS2), it undergoes a ring opening, first rearranging into isomer 83⁺ (II) and then fragmenting (TS3) into the ion $HCNH^+$ (m/z 28⁺) with the release of CO and HCN. In 5NI (Figure 3(b)), the 83⁺ ion also fragments by overcoming an energy barrier of only 1.14 eV (TS2), into CO and $HCNCHNH^+$ at m/z 55⁺ and then subsequently into the HCN molecule and the $HCNH^+$ ion at m/z 28⁺ via TS3. The analysis of the potential energy surfaces of 2NI (Figure 3(c)) shows a different scenario. In this case, the 83⁺ ion has to overcome a very large barrier of 2.75 eV (TS2) before the final fragmentation into HCN and CO molecules and the $HCNH^+$ ion can take place. This shows that, from the energetic point of view, the fragmentation of the 83⁺ intermediate is less favourable in 2NI than in the other isomers because the ring has a higher kinetic stability. Moreover, as can be observed in the mass spectra (Figure 1), the m/z 30⁺ peak is more intense in the 2NI isomer than in the 4NI and 5NI cases. This is because in 2NI the energy of 1.57 eV for the separation of NO^+ is lower than the barrier for the following fragmentation of m/z 83⁺, as shown in Figure 3. In the 4NI and 5NI isomers, the energy requirements are reversed, explaining the less intense m/z 30⁺ peak in their mass spectrum.

Additional support for these theoretical predictions is provided by the mass spectra measured at the photon energy of 16.67 eV (Ne I) of a rare gas discharge lamp (see the [supplementary material](#)).

These spectra show very asymmetric lineshapes for several features, giving clear evidence of metastable processes²⁹ leading to the formation of the m/z 83⁺ and 30⁺ fragments in 2NI as well as 28⁺ and 55⁺ in 4(5)NI, with a time scale in the order of several tens to hundred ns. This suggests, in agreement with the theoretical description, that molecular rearrangements and two-step fragmentation mechanisms are at the origin of those fragments. Such asymmetric lineshapes could not be observed in the experiments at Elettra due to the pulsed operation of the experimental setup, with the extraction of the ions switching on about 500 ns after the ionisation event (see the [supplementary material](#)).

In summary, the calculations show that all of the nitroimidazole isomers are likely to release NO with similar probability. However, in 4(5)NI the subsequent fragmentation of the residual m/z 83⁺ intermediate destroys the imidazole ring releasing HCN and CO molecules, while in 2NI the higher stability of the ring leaves the intermediate intact. These results explain the different intensity of the fragments at m/z 83⁺, 55⁺, 30⁺, and 28⁺ observed in both the mass spectra and PEPICO measurements.

In conclusion, the possible implications of our results in the context of radiosensitising mechanisms suggest that

the products of decomposition of the different nitroimidazole isomers might play a role in determining their distinctive degrees of effectiveness in radiotherapy. Nitric oxide, NO, which can be released by all nitroimidazole isomers with about equal probability, is a very reactive radical with a short lifetime and the possibility to diffuse freely across membranes that make it a powerful signalling molecule for vasodilation.^{9,10} Being released and active for a short while after irradiation and decomposition of the radiosensitisers, NO could have two actions, saturating dangling bonds in damaged DNA, making the damage permanent, and “favouring either drug delivery or the therapeutic efficacy of irradiation through transient tumour reoxygenation,” as suggested in Ref. 9. These effects, in addition to the redox mechanism, may provide the explanation of the potential of all nitroimidazoles as radiosensitisers active on hypoxic tumours.¹² On the other hand, the release of carbon monoxide, CO, and hydrogen cyanide, HCN, more pronounced in 4(5)NI isomers, may induce an opposite effect by efficiently attaching to haemoglobin³⁰ and inhibiting the cytochrome c oxidase³¹ in mitochondria, respectively, therefore effectively reducing the needed oxygenation and the overall radiosensitising effect. The importance of these processes when nitroimidazole derivate radiosensitizers operate in real biological media depends on how the bio-environment influences their energetics. However the understanding of the very basic chemical and physical mechanisms that determine the molecular response of cells and their building blocks to radiosensitising drugs is of fundamental importance to increase the potential of radiotherapy. Moreover, despite the fact that the typical energies used in radiotherapy are in the keV to MeV range, i.e., far above the VUV range explored in this work, the present results do not lose their potential impact in the context of radiotherapy because it is well documented^{4,32} that a large fraction of the radiation damage on biological systems is due to secondary processes releasing particles (electrons, ions, radicals) with a broad energy distribution, which can subsequently trigger the damaging of DNA and its surrounding environment.

See the [supplementary material](#) for detailed description of the experimental apparatuses and procedures, optimised geometries of parent ion and transition states, table of Electronic Energy (E_e) and Zero Point Energy (ZPE) of all the stationary points investigated, and intrinsic reaction coordinate calculations for the transition state TS1.

This work is partially supported by the XLIC COST Action CM1204 via the STSM program, the Serbia–Italy Joint Research Project “Nanoscale Insight in the Radiation Damage,” the MIUR FIRB RBFR10SQZI project 2010. H.S. acknowledges the receipt of a fellowship from the ICTP Programme for Training and Research in Italian Laboratories, Trieste, Italy. S.T. and B.P.M. acknowledge partial support of MESTD Project No. OI171020. M.M. acknowledges the Erasmus + EU program for support during her stay at the GasPhase beamline of Elettra-Sincrotrone Trieste.

We are very grateful to Mr. A. Morabito and Mr. S. Rinaldi for their excellent technical support with the experiments.

- ¹A. C. Begg, F. A. Stewart, and C. Vens, *Nat. Rev. Cancer* **11**, 239–253 (2011).
- ²M. M. Poggi, C. N. Coleman, and J. B. Mitchell, *Curr. Probl. Cancer* **25**, 334–411 (2001).
- ³P. Wardman, *Clin. Oncol.* **19**, 397–417 (2007).
- ⁴B. Boudaiffa, P. Cloutier, D. Hunting, M. A. Huels, and L. Sanche, *Science* **287**, 1658–1660 (2000).
- ⁵S. Rockwell, I. T. Dobrucki, E. Y. Kim, S. T. Marrison, and V. T. Vu, *Curr. Mol. Med.* **9**, 442–458 (2009).
- ⁶L. B. Harrison, M. Chadha, R. J. Hill, K. Hu, and D. Shasha, *Oncologist* **7**, 492–508 (2001).
- ⁷P. Howard-Flanders, *Nature* **180**, 1191–1192 (1957).
- ⁸L. H. Gray, F. O. Green, and C. A. Hawes, *Nature* **182**, 952–953 (1958).
- ⁹P. Sonveaux, B. F. Jordan, B. Gallez, and O. Feron, *Eur. J. Cancer* **45**, 1352–1369 (2009).
- ¹⁰P. Wardman, K. Rothkamm, L. K. Folkes, M. Woodcock, and P. J. Johnston, *Radiat. Res.* **167**, 475–484 (2007).
- ¹¹G. D. Wilson, S. M. Bentzen, and P. M. Harari, *Semin. Radiat. Oncol.* **16**, 2–9 (2006).
- ¹²G. S. Higgins, S. M. O’Cathail, R. J. Muschel, and W. G. McKenna, *Cancer Treat. Rev.* **41**, 105–113 (2015).
- ¹³W. R. Wilson and M. P. Hay, *Nat. Rev. Cancer* **11**, 393–410 (2011).
- ¹⁴R. R. Blyth, R. Delaunay, M. Zitnik, J. Krempasky, J. Slezak, K. C. Prince, R. Richter, M. Vondracek, R. Camilloni, L. Avaldi, M. Coreno, G. Stefani, C. Furlani, M. De Simone, S. Stranges, and M.-Y. Adam, *J. Electron Spectrosc. Relat. Phenom.* **101–103**, 959–964 (1999).
- ¹⁵P. Bolognesi, J. A. Kettunen, A. Cartoni, R. Richter, S. Tosic, S. Maclot, P. Rousseau, R. Delaunay, and L. Avaldi, *Phys. Chem. Chem. Phys.* **17**, 24063–24069 (2015).
- ¹⁶O. Plekan, M. Coreno, V. Feyer, A. Moise, R. Richter, M. De Simone, R. Sankari, and K. C. Prince, *Phys. Scr.* **78**, 058105 (2008).
- ¹⁷A. Cartoni, P. Bolognesi, E. Fainelli, and L. Avaldi, *J. Chem. Phys.* **140**, 184307 (2014).
- ¹⁸P. Jimenez, J. Laynez, R. M. Claramunt, D. Sanz, J. P. Fayet, M. C. Vertut, J. Catalàn, J. L. G. de Paz, G. Pfister-Guillouzo, C. Guimon, R. Flammang, A. Maquestiau, and J. Elguero, “The problem of the tautomerism of 4 (5)-nitroimidazole: A theoretical and experimental study,” *New J. Chem.* **13**, 151–156 (1989).
- ¹⁹A. I. Vokin, L. V. Sherstyannikova, I. G. Krivoruchka, T. N. Aksamentova, O. V. Krylova, and V. K. Turchaninov, *Russ. J. Gen. Chem.* **73**, 973–984 (2003).
- ²⁰L. Feketeová, O. Plekan, M. Goonewardane, M. Ahmed, A. L. Albright, J. White, R. A. J. O’Hair, M. R. Horsman, F. Wang, and K. C. Prince, *J. Phys. Chem. A* **119**, 9986–9995 (2015).
- ²¹See <http://www.nist.gov> for Data from NIST Standard Reference Database 69: NIST Chemistry WebBook; NIST MS number 235477.
- ²²P. Bolognesi, P. O’Keeffe, and L. Avaldi, “Soft x-ray interaction with organic molecules of biological interest,” in *Radiation Damage in Biomolecular Systems, Biological and Medical Physics, Biomedical Engineering*, edited by G. G. Gomez-Tejedor and M. C. Fuss (Springer Science+Business Media B.V., 2012).
- ²³M. J. Frisch, G. W. Trucks, H. B. Schlegel, G. E. Scuseria, M. A. Robb, J. R. Cheeseman, G. Scalmani, V. Barone, B. Mennucci, G. A. Petersson *et al.*, GAUSSIAN 09, Revision A.02, Gaussian, Inc., Wallingford, CT, 2009.
- ²⁴M. W. Wong, *Chem. Phys. Lett.* **256**, 391–399 (1996).
- ²⁵K. Raghavachary, G. W. Trucks, J. A. Pople, and M. A. Head-Gordon, *Chem. Phys. Lett.* **157**, 479–483 (1989).
- ²⁶T. J. Lee and P. R. Taylor, *Int. J. Quantum Chem.* **36**, 199–207 (1989).
- ²⁷C. Gonzalez and H. B. Schlegel, *J. Chem. Phys.* **90**, 2154–2161 (1989).
- ²⁸C. Gonzalez and H. B. Schlegel, *J. Phys. Chem.* **94**, 5523–5527 (1990).
- ²⁹D. Proch, D. M. Rider, and R. N. Zare, *Chem. Phys. Lett.* **81**, 430–434 (1981).
- ³⁰J. M. Berg, J. L. Tymoczko, and L. Stryer, *Biochemistry*, 7th ed. (W. H. Freeman and Company, 2012), ISBN 13: 9781429229364.
- ³¹S. Yoshikawa and W. S. Caughey, *J. Biol. Chem.* **265**, 7945–7958 (1990).
- ³²B. D. Michael and P. A. O’Neill, *Science* **287**, 1603–1604 (2000).